# Chirp Modulation Enabled Turbidity Measurement for Large Scale Monitoring of Fresh Water

Junxuan Wei[a], Fei Qin[a,*], Gang Li[b], Xujie Li[c], Xiaobo Liu[d], Xuewu Dai[e,*]

[a]*School of Electronic Electrical and Communication Engineering, University of Chinese Academy of Sciences, Beijing, China*
[b]*Information Center, Ministry of Water Resources of the People's Republic of China, Beijing, China*
[c]*College of Computer and Information, Hohai University, Nanjing, China*
[d]*Department of Water Ecology and Environment, China Institute of Water Resources and Hydro-power Research, Beijing, China*
[e]*Department of Physics and Electrical Engineering, Northumbria University, Northumbria, UK*

**Abstract**

Monitoring water turbidity accurately at a large scale provides vital information to alert abnormal water pollution event. However, scientists and engineers have to make the tradeoff among accuracy, range, and cost of turbidity measurement solutions. Consequently, the state of the art solutions utilize high-end hardware configurations to maintain high accuracy at wide dynamic range, which are either too expensive or complex to be adopted in large-scale monitoring. A low cost turbidity sensor without compromising on accuracy and dynamic range raises a big challenge. This paper approaches this challenge with Chirp modulation and signal convolution in the statistical domain, which can provide more than 40dB gain with traditional low-cost photodiode. The proposed solution can significantly increase the system performance scaled with hardware configurations. As a result, the implemented proof of concept system can provide as high as 2% measurement accuracy over a wide range of 0-1000 NTU with low-cost hardware configurations.

*Keywords:* Optical Turbidity measurement, Chirp modulation, Large scale monitoring, Wide range, Low-Cost
*2010 MSC:* 00-01, 99-00

## 1. Introduction

With the increasing restrictive requirements on water quality and tightening environmental standards, large scale water quality monitoring is needed to secure the protection on water resources and meet the demand on fresh water supplies. Among all water quality indicators, turbidity represents the presence of particles inside the water, including soil, colloidal, plankton etc. [1, 2, 3, 4]. As a result, the turbidity indicator has been widely utilized in water resource monitoring systems to detect the abnormal events, especially for natural water and drinking water [5]. Moreover, as the suspended particles in the water are usually acting as the carrier of pollutants, an accurate measurement of turbidity will significantly increase the efficiency to monitor many other water quality indicators, like Chemical Oxygen Demand (COD) [6]. Nonetheless, the promoting Internet of Things (IoT) for water resources can provide significantly increased performance of pollution monitoring, predication and footprint tracing, where large scale deployable turbidity sensors are necessary [7, 8]. Such a device for measuring turbidity is called turbidimeter, turbiditimeter, or turbidity meter. However, the traditional turbidimeter and its measurement methods were mainly designed for lab instruments rather than in-situ sensors. As a result, the traditional turbidity instruments are usually bulky, energy intensive and sometimes high-cost to achieve higher accuracy with complex architecture, tight requirement on working conditions and some times even manual operations [9]. Thus, most Commercial off the shelf (COTS) turbidity measurement products fail to satisfy the requirements for large scale monitoring of fresh waters [10, 11]. Consequently, many research efforts have been invested into the design of low cost, low power, high accuracy, and environment robust measurement method for turbidity in fresh water [11, 12, 13, 14].

Due to the scattering and possible absorption effects caused by the suspended particles in the water, the direction of the transmission light may varied significantly from its incident angle. According to which direction of light is used to measure the turbidity, there are mainly two types of turbidity measurement methods, known as *turbidimetry* measuring the transmission light and *nephelometry* measuring the scattering light[15, 16], shown in Fig. 1. According to the well-known Beer-Lambert law [17], the photon process inside the water will arise a paradox between these two measurement principles. For samples with low turbidities, the scattering intensities will be very small and hard to be detected since the signal might be lost in the electronics noise, while for samples with high turbidities, the intensity of transmission light will be very

*Corresponding authors
*Email addresses:* fqin1982@ucas.ac.cn (Xuewu Dai), xuewu.dai@northumbria.ac.uk (Xuewu Dai)

low and hard to be detected from noises. If the interference from ambient light, phase noise, and temperature drifting are also taken into account, the effective noise will be even higher and the measurement accuracy is harder to remain. As a result, most turbidity measurement methods are either high accuracy but only works with short range [18], or works with wide range but lower accuracy [19].

To address this problem, some researchers propose to utilize orthogonal optical arrangement to gain the benefits of both transmission and scattering mode [12], where a photodiode and a phototransisitor have been deployed with 90 degree separation to receive both transmitted light and scattered light concurrently. This method successfully achieves high accuracy with wide range in the trade with the increased optical and electronic system complexity. In another state of the art approach, a high-accuracy wide-range turbidity measurement system has been proposed with precise single photon detector [20], where the measurement of light intensities have been replaced by counting the number of received photon within the observation window. It is believed that the essential gain of this method is the extremely high resolution and sensitivity brought by the single photon detector[1]. Obviously, both methods approach the high-accuracy and wide-range turbidity measurement in the trade of substantial hardware configurations, which may not only be expensive and complex but also be environment sensitive limiting the larger scale remote deployment.

Nonetheless, the essential performance gain of single photon based method is from the increased sensitivity and lowered noise figure, which can be contributed by many other solutions rather than precise optical arrangements. In fact, digital signal modulation[21], optical pulse coding[22, 23], and the combination of both modulation and coding have been widely utilized in similar optical based measurement system to increase the effective Signal to Noise Ratio (SNR) [24]. If further consider that the digital processing capability has been widely enabled with extremely low cost nowadays, it is reasonable to improve the system performance in the digital domain instead of traditional analog domain. Hinted by this, this paper proposes an turbidity measurement solution with Chirp modulation over infrared LED. The convolution of received signals from optical arrangement with *a priori* Chirp signals in the digital domain will approach both increased resolution and effective SNR. This solution can also be understand to approach single photon system in the level of group of photons inside a Chirp signal through statistical processing, while the single photon based method works in the single photon level through precise single photon detector.

As a result, the proposed proof of concept turbidity measurement system achieves 2% accuracy over the range of 0-1000 NTU with single optical arrangement in transmission mode. All the utilized devices including infrared LED, photodiode, and MCU are low cost oriented, the overall cost of which can be restrained within 10$. As there is no sensitive devices utilized, the proposed solution is also environment friendly, which make it suitable for the large scale deployment in wireless enabled IoT system for water resource monitoring.

[1]The first method will be briefed as two optical path method for later discussion, while the later will be briefed as single photon method.

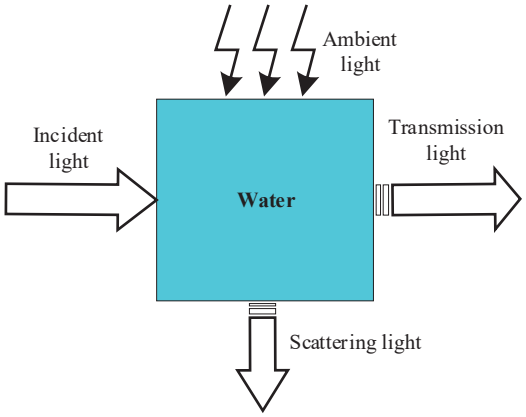


Figure 1: Incident light propagation model

The remaining of this paper is organized as follows. Section 2 presents the design principle and measurement method, as well as the structural overview of the system design are provided in section 3. Section 4 discusses the experiment setup and results. Section 5 will conclude this work with potential future works.

## 2. Measurement Principles

### *2.1. A. Principles of Turbidity Measurement with Noises*

The light propagation scheme inside the water is illustrated in Fig. 1, the incident light intensity is denoted as $I_0$, the received light intensity from transmission beam is denoted as $I_t$, and the light intensity of the scattering beam is denoted as $I_s$. Obviously, turbidity, denoted as $T$ in the following discussion, represents the optical clarity of the water and reflects how much the incident light is attenuated by the water and the suspended particles. Then, according to the well-known Beer-Lambert law [17], the relationship between the detected transmission light intensity $I_t$ and the turbidity $T$ can be modeled as follows:

$$I_t = k_1 I_0 e^{-\frac{1}{k_2}T}, \tag{1}$$

where $k_1$ and $k_2$ are the parameters of the model to be identified and varied in difference configurations, including light path, optical arrangement, temperature, substance and size of the suspended particles. This concept derived from [17] has been illustrated in the main part of Fig. 2. Given the incident light intensity $I_0$ is known and the intensity $I_t$ of the transmission light is measured by the optimal instrument, the turbidity $T$ can be estimated:

$$T = -k_2 \left(\ln I_t - \ln k_1 I_0\right). \tag{2}$$

In a turbidity measurement system, a photodetector, e.g. photodiodes, phototransistors, Avalanche photodiode (APD) and Photo-Multiplier Tubes (PMT), can be utilized to capture the transmitted or scattered light and convert the light photons into current with the photoemission effects. The current of photoelectrons induced in photoemission is then converted into voltage as well as necessary amplifier, which can be further mapped into digital domain with Analogue-to-Digital converters (ADC) for further process. Since the photon current in the photoemission process is proportional to the intensity of the detected light, the measured voltage is also propositional to the light intensity. Substitute the voltage $V_t$ that is proportional to the current $I_t$ into eq.(2), with simple algebra manipulation, the turbidity can be estimated from the obtained voltage:

$$T = -\beta_2 \left( \ln V_t - \beta_1 \right), \tag{3}$$

where $V_t$ represents the ADC output voltage, $\beta_1$ and $\beta_2$ are parameters to be identified. It is worth noting that the parameters $\beta_1, \beta_2$ (derived from $k_1$ and $K_2$) are usually hard to be analytically obtained due to the complex system configuration. Then, in the designed system, they will be identified through a series of calibration tests with pre-prepared standard samples with known $T$, i.e. the standard formazin [25]. This can be easily done by fitting of a series of known $T$ with the measured $V_t$. In ideal noise-free scenarios, the capture of $V_t$ plus pre-calibrated $\beta_1$,$\beta_2$ will lead to a high-accurate estimation of $T$. However, not only the photodetector and the electronic amplifiers suffer from various noises, e.g. shot noise, dark currents, leakage current and thermal noises, but also the ambient light is picked by the photodetector and works as an significant interference to the voltage measurements. Without loss of generality, the noise corrupted voltage can be modelled as a noisy representation of the intensity of transmission light:

$$V_t = \alpha I_t + n_o + n_e, \tag{4}$$

where $\alpha$ refers to the light-to-voltage conversion coefficients determined by the photodetector and amplification chain, $n_o$ denotes the optic noise introduced by both the ambient environment and photodetector, while $n_e$ is mainly contributed by the thermal noise in the electronic circuit. Beside of this, the environment changes may also cause the drifting of circuit working point, e.g. phase shifting, noise figure, and dark current. All of these factors will contribute to the uncertainties in the measurement model. As a result, it is hard to obtain an accurate model fitting, especially with non-linear exponential function existed for the transmission mode. The involved uncertainty will result in the poor performance at low turbidity region even with high received signal strength in the transmission mode.

In order to improve the accuracy of the turbidity measurement in the low turbidity region, some researchers propose the utilization of scattering light $I_s$, which can be approximated with linear function in the low turbidity region[12]. Similarly, this concluded concept has been illustrated in the insert in Fig. 2. With its linear form, the scattering based method can be simply calibrated in the analog domain, which can provide higher accuracy and reliability. In fact, the scattering light with 90 degree to the transmission beam, i.e. $I_{90}$, has been adopted in many standard of turbidity measurement [26]. However, with increased turbidity, the order of scattering will be increased as well. Then, the power of scattering light will be decreasing dynamically, as shown in the insert in Fig. 2. Consequently, not only the low SNR but also the break of monotone will make the scattering mode hard to be utilized in high turbidity region. It is then reasonable to design a hybrid system with dual optical arrangement to be benefited from both high accuracy in scattering mode and wide range in transmission mode as the work in [12]. Some work even proposes the involvement of more scattering paths than single $I_{90}$ to increase the system performance [27]. Without any doubts, the performance of these solutions are in the trade of system complexity especially the optical arrangement, which will increase the calibration efforts in the deployment.

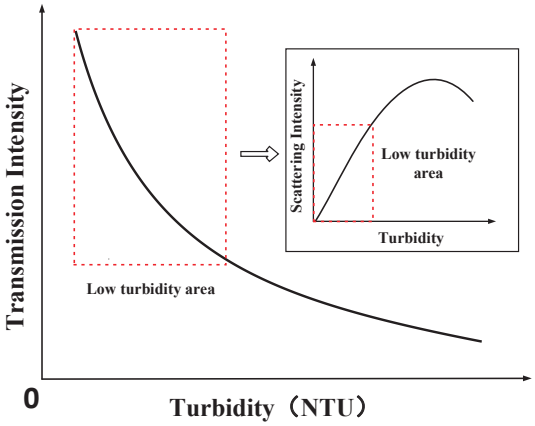


Figure 2: The relationship between light intensity and turbidity in the transmission mode and scattering mode

### 2.2. *Statistic Signal Processing for Accurate Turbidity Measurement*

While the same time, eq.(3) also reveals the fact that a wide-range and high-accuracy measurement system can be achieved with single transmission beam, as long as the uncertainty can be restrained. This has been demonstrated in [20, 28, 29], where a high precise single photon detector has been utilized to replace photodiode. Obviously, the performance gain of single photon based method is contributed in two folds, which has been concluded and illustrated in Fig. 3. The first is the extremely high resolution of single photon detector. Benefited by the single photon detector, the light intensity has been discretized into the precise photon level. Then, counting the photon numbers with an extremely high resolution will lead to an accurate

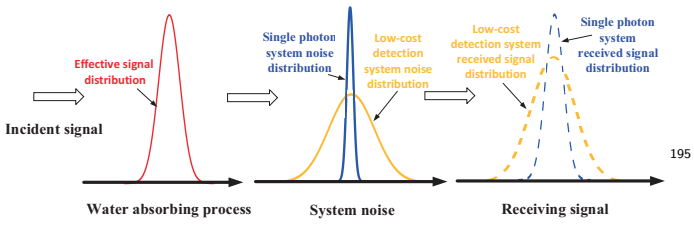


Figure 3: The statistical view of turbidity measurements

estimation in the statistical domain. The second fold is the significantly decreased noise. Nonetheless, the single photon detector is an electronic device, which will suffer from its measurement noise including dark count and after pulse effect [20]. However, the precise design and implementation of single photon detector can restrain such noise in an extremely low level. With these advantages, single photon detector based turbidity measurement system can achieve 5% high accuracy in a wide range of 0-1000 NTU, which is in the trade with substantial hardware overhead.

As discussed in the introduction, similar benefits in these two folds can be approached without precise devices. This paper utilizes Chirp modulation (or known as Linear Frequency Modulated Continuous Wave, LFMCW) over incident light intensity to approach this target [30], other solutions like Pseudo-Noise Coding may also apply [24]. In each transmission, a series of Chirp signals will be generated and modulated with infrared LED, which can be defined by:

$$s(t) = \sqrt{2}/2 p(t) \left[ e^{j\pi f(t)^2} + e^{-j\pi f(t)^2} \right], \qquad (5)$$

where $p(t)$ is a unit rectangular pulse function, $f$ represents the rate of change of frequency. Then, the frequency of Chirp will be linear with the increasing $t$.

In the receiver side, a homological copy of generated Chirp signal can be expected with delay, attenuation and noise:

$$r(t) = Ap(t) \left[ e^{j\pi f(t-t_d)^2} + e^{-j\pi f(t-t_d)^2} \right] + n, \qquad (6)$$

where $A$ is the averaged signal strength, $t_d$ denotes the propagation delay, $n$ represents all the involved noise. $t_d$ will be caused by both the light path and the electronic chain, which usually vary with the environment change and cause many troubles of calibration or fault detection. With the *a priori* information of generated Chirp signal, the received signal can be convoluted with local reference signal and get their cross-correlation in digital domain:

$$R(\tau) = \int_{-\infty}^{+\infty} r(t) S(\tau - t) dt. \qquad (7)$$

It worth noting that the Chirp signal is self orthogonal, therefore, all the expected light intensity will be concentrated on the output correlation peak located in $t_d$ of the digital domain. As the turbidity information is existed in the peak power, the variation of $t_d$ will not contribute to the uncertainty. Furthermore, as the noise $n$ is independent with the expected Chirp signal, the power of noise signal can be significantly reduced after the integration. This increases the system performance and approaches the single photon detector based system by lowering the effective noise.

Easy to know from eq.(7), the performance gain will be scaled with the length of $p(t)$, which is essentially applied on the bandwidth $\Delta f$ of modulated signal. Without any doubt, the larger bandwidth the higher performance gain can be noticed. Consequently, this will increase both the time and calculation cost. The complexity of eq.(7) is $O(n^2)$ with the calculation unit consisted by standard multiply and plus operation, which have been widely supported by modern embedded processor (e.g. even the low cost ARM Cortex M series employed in the following experiment). If considering that the correlation algorithm has been widely utilized in many research areas, numerous optimized algorithms have been proposed, which can achieve the complexity of $O(nlogn)$ [31]. As a result, the time cost of calculation will be much less than the time cost to transmit and receive modulated signal. In other word, the proposed algorithm is real time oriented.

Obviously, the photon scattering process inside the water is indeed a random process as well. As a result, the power of correlated peaks will be varied following a random distribution as well, which will involve the uncertainty. By deploying the Maximum Likelihood Estimation (MLE) over the correlated peaks, the value $R_{MLE}$ with the maximum statistical probability can be easily obtained, which is proportional to the light intensity with high resolution and accuracy. Then, eq.(3) can be rewrite as:

$$T = -\beta_2 \left( \ln R_{MLE} - \beta_1 \right). \qquad (8)$$

With the increased resolution and effective SNR, a significant improved measurement accuracy of turbidity can be expected over wide range. The next section will provide the design of a proof of concept system guided with this measurement principle.

## 3. System Design and Setup

As discussed in section 2, the performance gain of proposed system will be mainly contributed by the involved statistical processing, then the hardware design can be kept low-cost, low-power and small size oriented as shown in Fig. 4. Both the infrared LED HL-304IR3C-L3 [32] and the photodiode PD204-6C [33] are with a central wavelength of 940nm at a price of 0.2$/Pic, while the power consumption of which have been limited in mW level. As expected, most estimation work loads have now been moved to the statistical domain, which will require a signal processor. However, the computation cost is limited while not time sensitive. Then, a low cost MCU can be utilized,

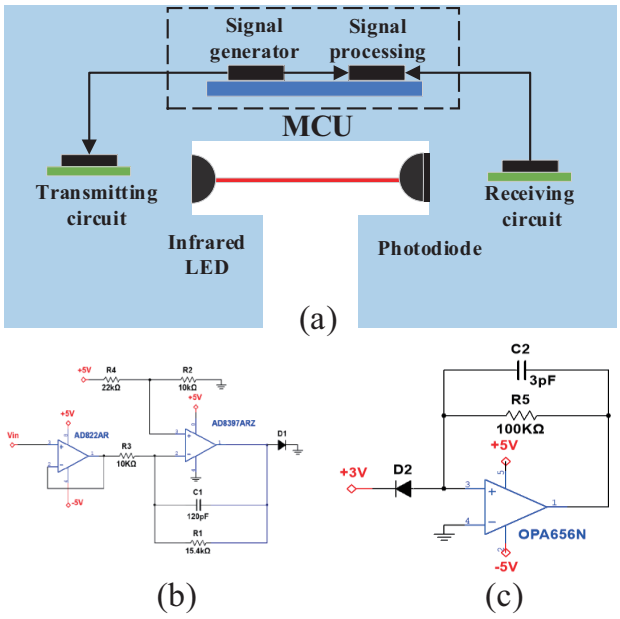


Figure 4: (a) The scheme of Turbidity measurement system, (b) Circuit design to drive infrared LED with DA in KL25z, (c) Circuit design of current to voltage mapping.

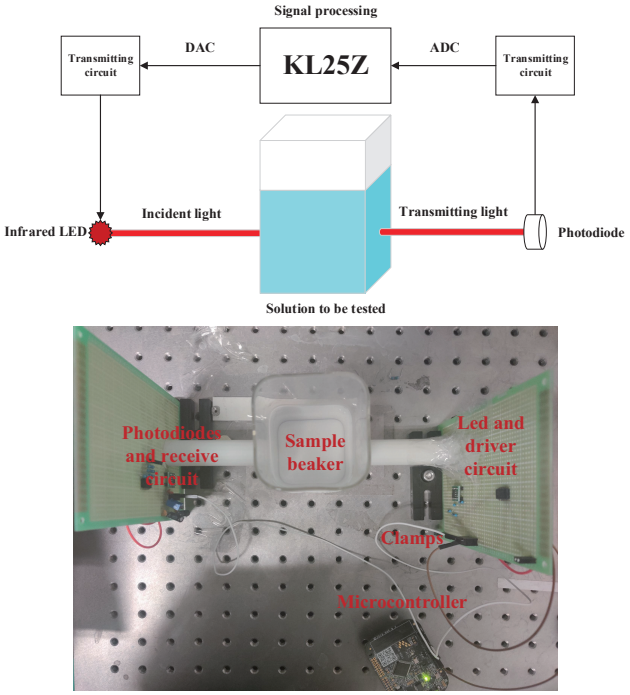


Figure 5: The scheme and photo of the proof of concept experiment


Figure 6: Reference turbidity testing instruments DR900 from HACH

i.e. KL25Z [34] based on simple Cortex-M0 has been employed in the proof of concept experiment with a price around 2$/pic. This MCU provides 32bit RISC architecture at 48MHz as well as a 12bit Digital Analog Converter (DAC) to drive the infrared LED with Chirp modulated signal. A 16 bit Analog Digital Converter (ADC) has been embedded as well to capture the received signal from photodiode. As shown in Fig. 4 (b), a voltage-current amplifier has been employed to drive the infrared LED with DA output in current, while an isolation circuit has been inserted before the amplifier in order to prevent the feeding back current. Similarly, the detected current of photodiode has been converted to the voltage with a trans-impedance amplifier, which will also provide a amplify gain for the detected signal. The overall BOM cost for this system can be restrained within 10$.

The test bench of the proof of concept system has been set up according to Fig. 5, where both the scheme and test photo have been provided. The transmitter unit has been firmly fixed in vertical on the optical platform, while the receiver unit has been fixed in parallel at the position opposite. Two 3D printed tubes have been employed to regulate the light beam to go through the test water in the beaker. The position of the square beaker has been accurately fixed on the optical platform throughout the process to avoid changes in the optical path, which may affect the calibration parameters.

As shown in Fig. 6, DR900 turbidmeter from HACH [35] was employed to provide the reference turbidity in the experiment, similar solutions of which has been utilized by [12] with different turbidmeters. DR900 is capable of measuring turbidity values in the range of 0-1000 NTU, and it is capable of providing an accuracy of 1 NTU. As a result, we only be able to provide results from 1-1000 NTU in the later experiment results section, which can be simply relaxed with a higher performance turbidmeter.

The turbidity solution samples were prepared by adding a standard 1000 NTU formazine solution to de-ionized water in the beaker. Then, the solution sample in the beaker was stirred to ensure homogeneity, and the actual turbidity was quickly tested using the DR900 turbidimeter with glass sample cell shown in Fig. 6. While the same time, the implemented proof of concept measurement system will be driven to measure the solution samples with series of modulated Chirp signals, the received signal will be captured and uploaded to the PC for later process, estimation and analyses. The solution needs to be stirred well before each experiment to prevent the suspended particles from set-

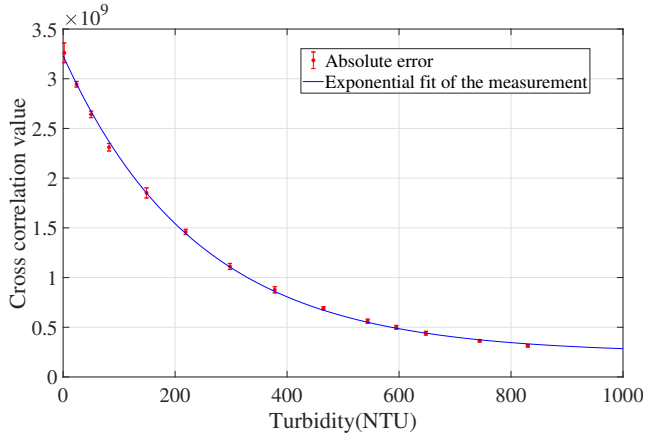


Figure 7: The estimated results in the range of 0-1000 NTU

| Sample | Turbidity (NTU) | Value ($10^9$) | Fitting Turbidity (NTU) | Relative error |
|---|---|---|---|---|
| 1 | 2 | 3.2603 | -2.3 | N/A |
| 2 | 24 | 2.9449 | 24.3 | 1.25% |
| 3 | 50 | 2.6414 | 52.9 | 5.80% |
| 4 | 82 | 2.3113 | 86.1 | 5.00% |
| 5 | 149 | 1.8514 | 148.8 | 1.30% |
| 6 | 219 | 1.4591 | 215.9 | 1.42% |
| 7 | 298 | 1.1123 | 296.1 | 0.64% |
| 8 | 378 | 0.87639 | 372.5 | 1.46% |
| 9 | 465 | 0.69094 | 455.7 | 2.00% |
| 10 | 544 | 0.56082 | 537.0 | 1.29% |
| 11 | 595 | 0.49933 | 588.4 | 1.11% |
| 12 | 648 | 0.44041 | 648.2 | 0.03% |
| 13 | 744 | 0.36358 | 760.5 | 2.22% |
| 14 | 830 | 0.31258 | 860.5 | 3.67% |

Table 1: The comparison between detection results and turbidity in the range of 0-1000 NTU

tling over time and affecting the measurement results.

## 4. Experimental results and discussion

The proposed measurement scheme discussed above has been utilized to process the received signals. Ten sets of data have been collected for each turbidity solution sample during the measurement process. Each set of data contains a series of 15 Chirp modulated signals, which refers a typical$\Delta f = 1000Hz$ has been chosen with 2000 sample points for each Chirp. The statistical estimation of these data sets was used as the experimental value for correlation fitting. The results of which will be shown in the following discussion.

As shown in Fig. 7, the proposed solution achieves an ideal exponential fitting with reference turbidity provided by DR900 in a wide range of 0-1000 NTU. As detailed in Table 1, in total 14 samples have been tested ranging from 2 NTU to 830 NTU. The obtained correlation coefficient, i.e. $R^2$ is 0.9993, which shows comparable results of single photon detector based solution with $R^2 = 0.9912$ and two optical arrangement solution with $R^2 = 0.9936$ both for NTU ranging 0-1000. The relative error for each measurements have been provided in Table 1 as well as illustrated with error bar in Fig. 7. Similarly, an overall high accuracy has been obtained with average relative error of 2.07%, which is slightly better comparing with 5% relative error for the single photon solution and 20% relative error for the two optical arrangement solution for 0-1000NTU, which shows significantly increased performance. For sample 3 and 4, the relative errors are slightly high at 5.8% and 5%, which may due to the non-calibrated environment issues like temperature or the accidental moving of beaker.

To further provide details of statistical based estimation, the captured Chirp signals as well as the statistical results have been illustrated in Fig. 8. The results of four samples have been provided, i.e. 744 NTU, 219 NTU, 82 NTU, and 2 NTU, while the raw Chirp correlations was only provided for 219 NTU to save space. As expected,

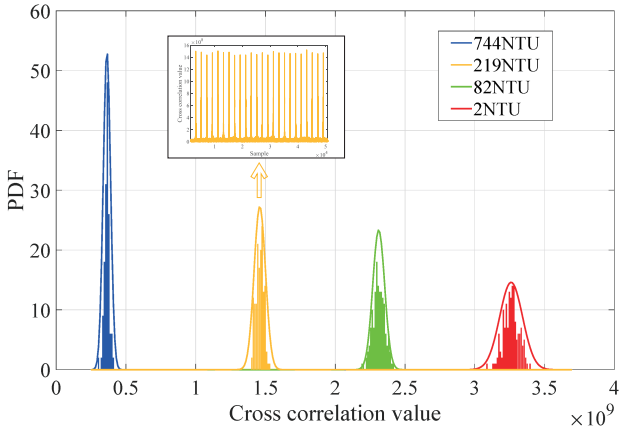


Figure 8: Statistical distribution of cross-correlation results at 2, 82, 219 and 744 NTU

the involvement of Chirp modulation enables the statistical information with the equalized discretization. The outputs of convolution over Chirp signals have all shown good match with Possion distribution. As revealed by the discussion in section 2, although the raw amplitude is high for the samples with low turbidity, the variations will be high to cause uncertainty, which will be significantly amplified in the analog domain. And for the samples with high turbidity, the variation is limited even with low amplitudes. In addition, these results also reveal the fact that the measurement time can be dynamically controlled for different turbidity levels, and in the low turbidity region, more interdependent single pulse peaks can be counted, which can improve the measurement accuracy more effectively.

In Fig. 9, the statistical distribution of relative errors from both the Chirp modulation method and the two optical path method have been provided for the same turbidity sample with NTU of 424. The results were captured with strictly the same hardware configuration. The transmitted signal was modulated with Chirp signal in the proposed method, while the raw signal was transmitted and cap-

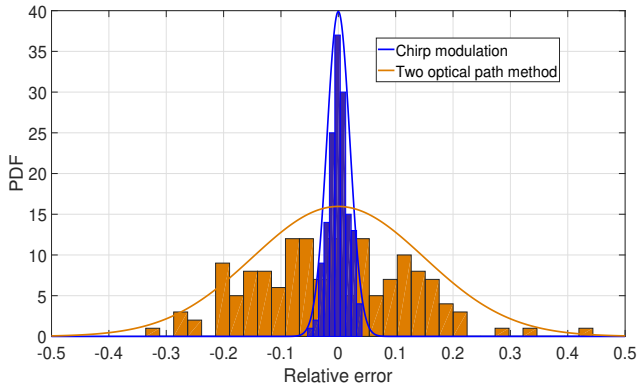


Figure 9: Statistical distribution of relative error for the chirp modulation and two optical path method

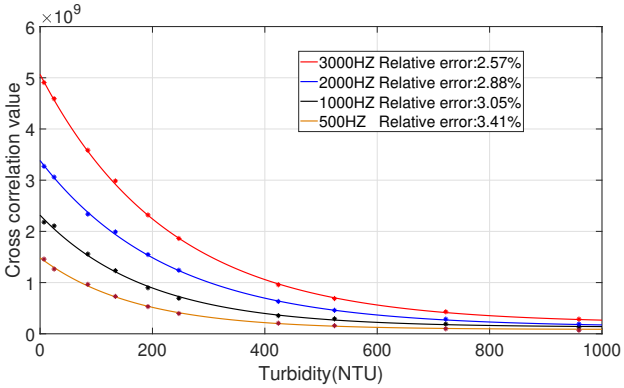


Figure 11: The estimated results in the range of 0-1000 NTU with different Chirp configurations

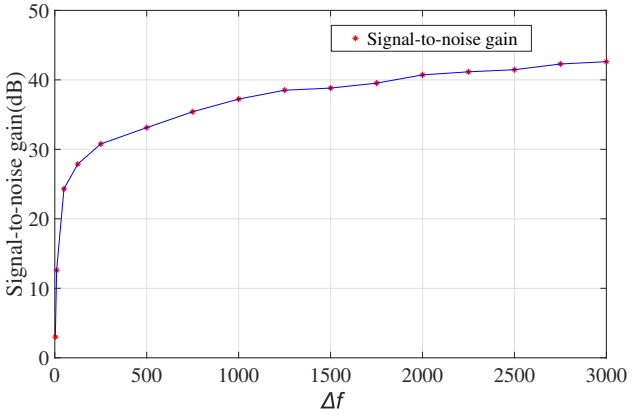


Figure 10: The relationship between $\Delta f$ and signal-to-noise gain

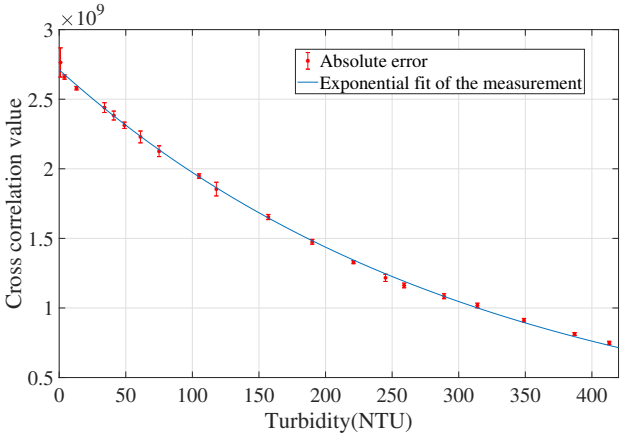


Figure 12: The estimated results in the range of 0-400 NTU

tured in the two optical path method following [12]. The relative error is employed due to the significant quantitative difference between the correlation result from Chirp modulation and raw result from two optical path method. As expected in the discussion of Fig. 3, the $\sigma$ of the Chirp modulation method is only 0.017, which is much smaller than 0.162 of the two optical path method. Obviously, these results confirms that the uncertainty of turbidity measurement can be attenuated leading to increased accuracy.

As discussed in section II, the expected performance gain will be contributed by the increased effective SNR, which have been shown in Fig. 10. In Fig. 10, the transmission Chirp signal has been varied with varying length $p(t)$, which will resulted in the varying frequency change denoted with $\Delta f$ in the figure. The signal-to-noise gain was calculated by the ratio between raw received signal and convoluted signal. With $\Delta f$ degraded to zero, the proposed system will be back compatible as DC monitoring in the analog domain. In the other side, the performance gain tends to converge with larger $\Delta f$, i.e. a stationary performance gain around 40dB can be expected for most $\Delta f$ from 500Hz to 3000Hz, which infers the capability bound of this method. Even though, a significant performance gain can be expected even with small $\Delta f$.

In order to verify the relationship between signal-to-noise gain and $\Delta f$. We selected $\Delta f$ = 500HZ, 1000HZ, 2000HZ, 3000HZ for the four sets of experiments, while each set contains 10 samples within 0-1000NTU. The results have been shown in Fig. 11. As expected, there is a good exponential relationship between the cross correlation value and the turbidity in all configurations. More importantly, the relative error of the measurement results will decrease with the increasing $\Delta f$, which indicates that a higher $\Delta f$ will guarantee higher measurement accuracy but with longer measurement time and processing cost. Considering both measurement accuracy and measurement time, a typical $\Delta f$ = 1000Hz has been chosen in our experiments.

In order to verify the performance of turbidity detection in the low concentration region within 0-400 NTU. Another experiments with newly prepared 20 turbidity solution samples have been deployed in Fig. 12 and table 2. Strictly the same device and processing algorithms have been implemented as the experiment for 0-1000NTU, i.e. nothing changed except the turbidity samples. As expected, the proposed solution also shows an ideal exponen-

tial fitting with reference turbidity provided by DR900 in the range of 0-400 NTU. As detailed in Table 2, in total 20 samples has been tested ranging from 1 NTU to 413 NTU. The obtained correlation coefficient, i.e. $R^2 = 0.9989$, while the two optical arrangement solution achieves $R^2 = 0.9981$ in the low concentration region[2]. The relative errors for each measurement have been provided in Table 2 as well as illustrated with error bar in Fig. 12. Similarly, an overall high accuracy has been obtained with average relative error of 2.73%, which is also comparable with 2.03% for the experiment ranging from 0-1000 NTU. The two optical arrangement solution achieves 10% with similar experiment configuration. Similarly, two unexpected large results can be noticed for sample 2 and 4, where the relative error are as large as 7.50% and 8.82%, which may also due to precision of reference turbidity from DR900.

| Sample | Turbidity (NTU) | Value ($10^9$) | Fitting Turbidity (NTU) | Relative error |
|---|---|---|---|---|
| 1 | 1 | 2.7640 | -5.5 | N/A |
| 2 | 4 | 2.6590 | 3.7 | 7.50% |
| 3 | 13 | 2.5792 | 13.3 | 2.30% |
| 4 | 34 | 2.4397 | 31.0 | 8.82% |
| 5 | 41 | 2.3826 | 38.6 | 5.85% |
| 6 | 49 | 2.3128 | 47.9 | 2.24% |
| 7 | 61 | 2.2290 | 59.5 | 2.45% |
| 8 | 75 | 2.1263 | 74.5 | 0.67% |
| 9 | 105 | 1.9478 | 102.5 | 2.38% |
| 10 | 118 | 1.8543 | 117.7 | 0.25% |
| 11 | 157 | 1.6535 | 153.7 | 2.10% |
| 12 | 190 | 1.4757 | 189.8 | 0.11% |
| 13 | 221 | 1.3291 | 222.8 | 0.81% |
| 14 | 245 | 1.2166 | 250.7 | 2.33% |
| 15 | 259 | 1.1617 | 265.4 | 2.47% |
| 16 | 289 | 1.0942 | 283.8 | 1.80% |
| 17 | 314 | 1.0277 | 303.8 | 3.25% |
| 18 | 349 | 0.91189 | 342.0 | 2.01% |
| 19 | 387 | 0.81317 | 377.2 | 2.53% |
| 20 | 413 | 0.74887 | 404.4 | 2.08% |

Table 2: The comparison between detection results and turbidity in the range of 0-400 NTU

## 5. Conclusion and Future works

This paper first analyses the existing method for optical turbidity measurements, where a comprehensive system model has been set to explain the essential motivations of the state of the art turbidity measurement solutions. This model also hints us to introduce modern digital signal processing algorithms to enable the statistical estimation for significantly increased performance of turbidity measurement.

Following these principles, a proof of concept system has been designed and implemented with Chirp modulation. The overall BOM cost for the proposed system can be restrained within 10$, while the measurement performance approaching the state of the art turbidity measurement solution designed for high-accuracy and wide range measurement, shown in Table 3. This, without any doubt, reveals the possibility of realizing a low-cost, high-accuracy, wide-range turbidity measurement system for the large scale monitoring of fresh water.

| Method | Accuracy | R-squared |
|---|---|---|
| Chirp modulation | 2% in 0-1000NTU | 0.9993 in 0-1000NTU |
| Single photon method[20] | 5% in 0-1000NTU | 0.9912 in 0-1000NTU |
| Two optical path method[12] | 15% in 0-1000NTU | 0.9936 in 0-1000NTU |

Table 3: Comparison of different turbidity testing methods

According to the similar principle, other important water quality indicators, e.g. Chemical Oxygen Demand (COD), Total Organic Carbon (TOC), and Total Nitrogen (TN) etc., can also be expected with low-cost and high accuracy architecture, which will be discussed in our future works.

[2]No comparable experiment has been deployed in single photon detector base solution.


## Acknowledgement

This work is supported by the Fundamental Research Funds for the Central Universities, in part by Open Research Fund Key Laboratory of Wireless Sensor Network and Communication, Chinese Academy of Sciences under Grant 20190914, in part by the Provincial Key Research and Development Program of Jiangsu under Grant BE2019017, and in part by the Provincial Water Science and Technology Program of Jiangsu under Grant 2020028.


## References


[1] D. Chapman, Water quality assessments : a guide to the use of biota, sediments, and water in environmental monitoring, Chapman & Hall, 1992.

[2] B. G. Kitchener, J. Wainwright, A. J. Parsons, A review of the principles of turbidity measurement, Progress in Physical Geography: Earth and Environment 41 (5) (2017) 620–642. doi:10.1177/0309133317726540.

[3] R. J. Davies-Colley, D. G. Smith, Turbidity, suspended sediment, and water clarity, Jawra Journal of the American Water Resources Association 37 (5) (2001) 1085–1101.

[4] B. G. B. Kitchener, S. D. Dixon, K. O. Howarth, A. J. Parsons, J. Wainwright, M. D. Bateman, J. R. Cooper, G. K. Hargrave, E. J. Long, C. J. M. Hewett, A low-cost bench-top research device for turbidity measurement by radially distributed illumination intensity sensing at multiple wavelengths, HardwareX 5.

[5] J. Downing, Turbidity Monitoring, John Wiley & Sons, Inc., 2005.

[6] X. Dai, S. J. Sheard, D. O'Brien, S. Russell, L. Carswell, Propagation and scattering model of infrared and ultraviolet light in turbid water, in: 22nd Wireless and Optical Communication Conference, 2013, pp. 601–606. doi:10.1109/WOCC.2013.6676445.

[7] J. Bhardwaj, K. K. Gupta, R. Gupta, A review of emerging trends on water quality measurement sensors, in: International Conference on Technologies for Sustainable Development (ICTSD), 2015, pp. 1–6. doi:10.1109/ICTSD.2015.7095919.

[8] V. Raut, S. Shelke, Wireless acquisition system for water quality monitoring, in: 2016 Conference on Advances in Signal Processing (CASP), 2016, pp. 371–374. doi:10.1109/CASP.2016.7746198.

[9] O. Korostynska, A. Mason, A. I. Al-Shamma'a, Monitoring Pollutants in Wastewater: Traditional Lab Based versus Modern Real-Time Approaches, Springer Berlin Heidelberg, Berlin, Heidelberg, 2013, pp. 1–24. doi:10.1007/978-3-642-37006-9_1.

[10] S. Panguluri, G. Meiners, J. Hall, J. G. Szabo, Distribution system water quality monitoring: Sensor technology evaluation methodology and results. environmental protection agency, washington, dc.

[11] A. A. Azman, M. H. F. Rahiman, M. N. Taib, N. H. Sidek, I. A. Abu Bakar, M. F. Ali, A low cost nephelometric turbidity sensor for continual domestic water quality monitoring system, in: IEEE International Conference on Automatic Control and Intelligent Systems (I2CACIS), 2016, pp. 202–207. doi:10.1109/I2CACIS.2016.7885315.

[12] Y. Wang, S. M. S. M. Rajib, C. Collins, B. Grieve, Low-cost turbidity sensor for low-power wireless monitoring of fresh-water courses, IEEE Sensors Journal 18 (11) (2018) 4689–4696. doi:10.1109/JSEN.2018.2826778.

[13] S. Sendra, L. Parra, V. Ortuño, J. Lloret, A low cost turbidity sensor development, in: The Seventh International Conference on Sensor Technologies and Applications, 2013, pp. 260–265.

[14] O. L. Yashon O. Ouma, J. Waga, D. Mbuthia, Estimation of reservoir bio-optical water quality parameters using smartphone sensor apps and landsat ETM+: Review and comparative experimental results, Journal of Sensors 2018. doi:https://doi.org/10.1155/2018/3490757.

[15] J. Bratby, Chapter sixteen - turbidity : Measurement of filtrate and supernatant quality, in: S. Tarleton (Ed.), Progress in Filtration and Separation, Academic Press, Oxford, 2015, pp. 637–657. doi:https://doi.org/10.1016/B978-0-12-384746-1.00016-1.

[16] L. Xinterhofer, S. wardeaw, P. Jatlow, D. Seligson, Nephelometric determination of pancreatic enzymes: I.amylase, Clinica Chimica Acta 43 (1) (1973) 5 – 12. doi:https://doi.org/10.1016/0009-8981(73)90110-1.

[17] L. Wind, W. W. Szymanski, Quantification of scattering corrections to the beer-lambert law for transmittance measurements in turbid media, Measurement Science and Technology 13 (3) (2002) 270–275. doi:10.1088/0957-0233/13/3/306.

[18] T. P. Lambrou, C. C. Anastasiou, C. G. Panayiotou, M. M. Polycarpou, A low-cost sensor network for real-time monitoring and contamination detection in drinking water distribution systems, IEEE Sensors Journal 14 (8) (2014) 2765–2772. doi:10.1109/JSEN.2014.2316414.

[19] A. Garcia, M. A. Perez, G. J. G. Ortega, J. T. Dizy, A new design of low-cost four-beam turbidimeter by using optical fibers, IEEE Transactions on Instrumentation and Measurement 56 (3) (2007) 907–912. doi:10.1109/TIM.2007.894222.

[20] H. Wang, J. Hu, W. Wan, H. Gui, F. Qin, F. Yu, J. Liu, L. Lü, A wide dynamic range and high resolution all-fiber-optic turbidity measurement system based on single photon detection technique, Measurement 134 (2019) 820–824. doi:https://doi.org/10.1016/j.measurement.2018.12.012.

[21] D. Zhou, Y. Dong, B. Wang, C. Pang, D. Ba, H. Zhang, Z. Lu, H. Li, X. Bao, Single-shot botda based on an optical chirp chain probe wave for distributed ultrafast measurement, Light: Science & Applications 7. doi:10.1038/s41377-018-0030-0.

[22] F. Wang, C. Zhu, C. Cao, X. Zhang, Enhancing the performance of botdr based on the combination of fft technique and complementary coding, Opt. Express 25 (4) (2017) 3504–3513. doi:10.1364/OE.25.003504.

[23] M. D. Jones, Using simplex codes to improve otdr sensitivity, IEEE Photonics Technology Letters 5 (7) (1993) 822–824. doi:10.1109/68.229819.

[24] X. Sun, Z. Yang, X. Hong, S. Zaslawski, S. Wang, M. A. Soto, X. Gao, J. Wu, L. Thévenaz, Genetic-optimised aperiodic code for distributed optical fibre sensors, Nature communications 11 (1) (2020) 5774. doi:10.1038/s41467-020-19201-1.

[25] L. Wind, W. W. Szymanski, Quantification of scattering corrections to the beer-lambert law for transmittance measurements in turbid media, Measurement Science and Technology 13 (6) (2002) 951–951. doi:10.1088/0957-0233/13/6/501.

[26] EN ISO 7027-1-2016, IX-CEN, 2016-06.

[27] T. Matos, C. L. Faria, M. S. Martins, R. Henriques, L. M. Goncalves, Development of a cost-effective optical sensor for continuous monitoring of turbidity and suspended particulate matter in marine environment, Sensors 19 (20) (2019) 4439.

[28] H. Wang, Y. Yang, Z. Huang, H. Gui, Instrument for real-time measurement of low turbidity by using time-correlated single photon counting technique, IEEE Transactions on Instrumentation and Measurement 64 (4) (2015) 1075–1083. doi:10.1109/TIM.2014.2364703.

[29] Y. Yang, H. Wang, Y. Cao, H. Gui, J. Liu, L. Lu, H. Cao, T. Yu, H. You, The design of rapid turbidity measurement system based on single photon detection techniques, Optics Laser Technology 73 (2015) 44 – 49. doi:https://doi.org/10.1016/j.optlastec.2015.04.005.

[30] T. K. LEE, K. YANG, Cross-correlation properties of generalized chirp-like sequences and their application to zero-correlation zone sequences, IEICE Transactions on Fundamentals of Electronics, Communications and Computer Sciences E97.A (12) (2014) 2549–2555. doi:10.1587/transfun.E97.A.2549.

[31] D. M. Tsai, C. T. Lin, Fast normalized cross correlation for defect detection, Pattern Recognition Letters 24 (15) (2003) 2625–2631.

[32] Hl-304ir3c-l3 user's manual, Tech. rep., HONGLI (2016). URL http://www.honglitronic.com

[33] Pd204-6c user's manual, Tech. rep., YIGUANG (2016). URL https://www.everlight.com

[34] Frdm-kl25z datasheet, Tech. rep., FREESCALE (2013). URL https://www.nxp.com

[35] Dr900 datasheet, Tech. rep., HACH (2016). URL https://www.hach.com.cn/product/dr900